OEDGE MODELING OF THE DIII-D H-MODE $^{13}CH_4$ PUFFING EXPERIMENT

by

J.D. ELDER, A.G. MCLEAN, P.C. STANGEBY, S.L. ALLEN,
J.A. BOEDO, B.D. BRAY, N.H. BROOKS, M.E. FENSTERMACHER,
M. GROTH, A.W. LEONARD, D. REITER, D.L. RUDAKOV,
W.R. WAMPLER, J.G. WATKINS, W.P. WEST, D.G. WHYTE

GENERAL ATOMICS

DISCLAIMER

GA–A25455

OEDGE MODELING OF THE DIII-D H-MODE 13CH4 PUFFING EXPERIMENT

by

J.D. ELDER,* A.G. MCLEAN,* P.C. STANGEBY,* S.L. ALLEN,[†]
J.A. BOEDO,[‡] B.D. BRAY, N.H. BROOKS, M.E. FENSTERMACHER,[†]
M. GROTH,[†] A.W. LEONARD, D. REITER,[§] D.L. RUDAKOV,[‡]
W.R. WAMPLER,[£] J.G. WATKINS,[£] W.P. WEST, D.G. WHYTE[ƒ]

*University of Toronto Institute for Aerospace Studies, Toronto,Canada
[†]Lawrence Livermore National Laboratory, Livermore, California
[‡]University of California, San Diego, California
[§]Forschungszentrum Juelich, GmbH 52425, Juelich, Germany
[£]Sandia National Laboratory, Albuquerque, New Mexico
[ƒ]University of Wisconsin, Madison, Wisconsin

GENERAL ATOMICS PROJECT 30200
JUNE 2006

GENERAL ATOMICS

ABSTRACT

Use of carbon in tokamaks leads to a serious tritium retention issue due to co-deposition. To further investigate the processes involved, a detached ELMy H-mode (6.5 MW NBI) experiment was performed on DIII-D in which $^{13}CH_4$ was puffed into the main vessel through the toroidaly symmetric pumping plenum at the top of lower single-null discharges. Subsequently, the ^{13}C content of tiles taken from the vessel wall was measured. The interpretive OEDGE code was used to model the results. The ^{13}C deposition pattern could be reproduced, in general shape and magnitude, by assuming in the code the existence of a parallel flow and a radial pinch in the scrape-off layer. Parallel flows of Mach ~ 0.3 toward the inner divertor and a radial pinch ~ 10 to 20 m/s ($+ R$-direction) were found to yield ^{13}C deposition comparable to the experiment.

1. INTRODUCTION

The carbon-hydrogen co-deposition process does not saturate and could result in an unacceptable buildup of tritium inventory in next-generation fusion devices. Three principal questions are involved: (1) What is the source of the carbon? (2) What transport process carries the carbon in the scrape-off layer (SOL)? (3) What determines the ultimate deposition location of the carbon? This paper is an interpretive modeling investigation related to the second and third questions in the context of a DIII-D H-mode $^{13}CH_4$ puffing experiment.

The injection of $^{13}CH_4$ into the edge of tokamaks has been shown on TEXTOR [1], JET [2] and DIII-D [3] to provide valuable opportunities for diagnosis of carbon behavior. In a previous experiment on DIII-D, $^{13}CH_4$ was puffed into a set of repeat, well-controlled, low power, ~1 MW, L-mode discharges. The resulting spectroscopic measurements and deposition pattern were successfully modeled [4,5]. In the present case, $^{13}CH_4$ was puffed through the upper pumping plenum into lower single-null (LSN), neutral beam heated (6.5 MW), detached ELMy H-mode discharges. The objective of the experiment was to measure the ^{13}C deposition under plasma conditions relevant to next-generation fusion devices.

The puff was toroidally symmetric through the upper pumping plenum into the crown of the plasma at a rate which did not significantly perturb the local plasma conditions. The average puff rate was 18.8 Torr-L/s lasting 2 s during each of 18 consecutive discharges. This flow rate was 4.3 times that used in the L-mode experiment and injected a total of 2.3 times as much ^{13}C into the plasma.

After this experiment, DIII-D was vented and a total of 77 tiles were removed. The ^{13}C content of 64 of the tiles was measured using nuclear reaction analysis [6,7]. ^{13}C deposition was found primarily on tiles in the inner divertor region and the private flux region with some measurable deposition near the puff region.

The OSM Eirene Divimp edge (OEDGE) code [8] was used in this study to model the breakup, transport and deposition of the puffed $^{13}CH_4$. The objective was to identify and quantify mechanisms that could lead to the measured ^{13}C deposition pattern. The key controlling physical processes found in the modeling are parallel flow toward the inner divertor and a radial pinch in the main SOL. To model this experiment, the OEDGE code was significantly enhanced by the addition of the Janev-Reiter database [9,10] of methane breakup processes as well as a completely revised and energetically consistent model for the molecular breakup kinetics.

2. RESULTS

The first step in the OEDGE analysis was to use all available experimental data and the "onion-skin" modeling (OSM) in OEDGE to infer a solution for the background plasma by empirical reconstruction [4,11]. This plasma solution (identified as OSM in the figures) is then used as the basis for calculating the transport and deposition of the ^{13}C in the rest of the study. Divertor Thomson System (DTS) measurements of n_e and T_e in the private flux zone (PFZ) and outer divertor were directly used to specify the plasma solution in these regions. In addition, the solution was also constrained to match additional experimental data including calibrated spectroscopic measurements of D_α and D_γ [from the Tangential Television (TTV) cameras as well as the Multichord Divertor Spectrometer (MDS)] for both the inner and outer targets, target Langmuir probe measurements of I_{sat}^+ and Thomson measurements of the plasma profiles both upstream (Fig. 1) and in the divertor. The solution matched the hydrogenic spectroscopy (EIRENE-calculated profiles) at the inner (Fig. 2) and outer targets. The inner target was found to be detached with a near target plasma temperature of 0.8 ± 0.2 eV. The outer target was also cold with a temperature ~ 2 eV. Superimposed by the code on the plasma solution was a parallel flow toward the inside of specified Mach number, $M_\parallel$. $M_\parallel \equiv v_\parallel /[(T_e + T_i)/m_D]^{1/2}$, $T_i = T_e$ assumed. In addition to a parallel flow, a radial pinch was found to be necessary to carry C ions produced from the CH$_4$ breakup toward the separatrix. This pinch was applied to the ions in the SOL above the X-point.
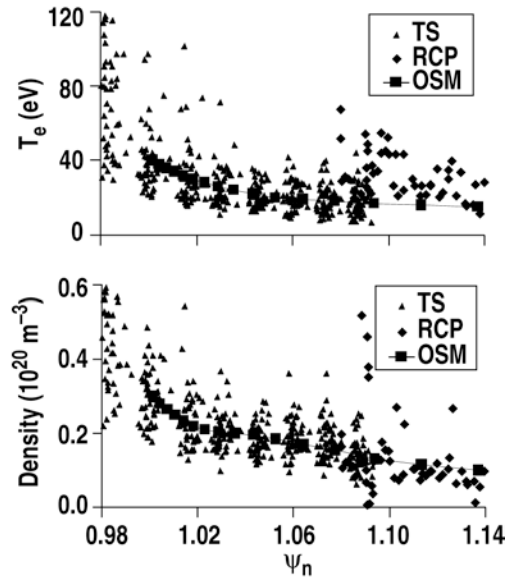

Fig. 1. Comparison of upstream n_e and T_e from Thomson (TS), reciprocating probe (RCP), and the OSM solution for the ^{13}C H-mode experiment.
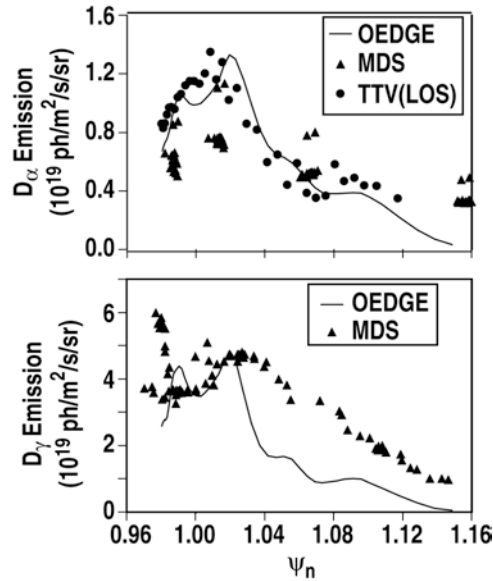
Fig. 2. Comparison of the experimental and modeled D_α, and D_γ spectroscopy at inner target. The modeled hydrogen spectroscopy is produced by EIRENE using the OSM plasma solution as input.

The essential difference in the deposition between the H-mode experiment and the previous L-mode experiment is the significant deposition in the PFZ seen in H-mode that is not seen in L-mode. The physics processes in the ELMy H-mode plasmas are more complex than in the L-mode plasmas. The ELMs occurred every ~ 5 ms with a duration of 2 to 3 ms as measured by D_α spectroscopy, line average density and target Langmuir probes. The ELMs involve time varying plasma conditions possibly including periodic changes in the plasma flows. Unfortunately, there were no measurements of local plasma flow speed. If ELMs play a direct role in the ^{13}C transport, then the most likely mechanism would appear to be changes to the spatial extent of the plasma flow as the result of the ELMs. This study thus examines two distinct transport hypotheses leading to the ^{13}C deposition – ELM-dependent and ELM-independent transport. In the ELM-dependent case, the ELMs are assumed to deposit sufficient energy in the inner divertor to move the ionization front and thus the parallel flow field towards the divertor target. Between ELMs, the parallel flow is hypothesized to stop near the entrance to the cold, stagnant inner divertor. In the ELM-independent case, the plasma flow conditions are assumed constant. It is hypothesized here, and discussed below, that erosion and redeposition of the ^{13}C depositing on the target is not significant. These two cases and the effects of extreme flow assumptions are reported next.

2.1. HYPOTHESIS 1: ELM-DEPENDENT TRANSPORT

Two simulation cases were analyzed. The first case assumes a parallel flow which ends near the entrance of the inner divertor. The second case assumes that the parallel flow

extends almost to the target plates. Both cases assume a radialy constant parallel flow at $M_{\parallel}$ = 0.3 and a radial pinch of 20 m/s. Deposition on the inner target mainly occurred when the flow extended into the inner divertor while the deposition in the PFZ mainly occurred when the flow stopped outside the inner divertor. A reasonable match to the experimental data, both as to shape and magnitude, is achieved by combining 50% of each profile, corresponding to the ELM on/off times being ~ equal (Fig. 3).
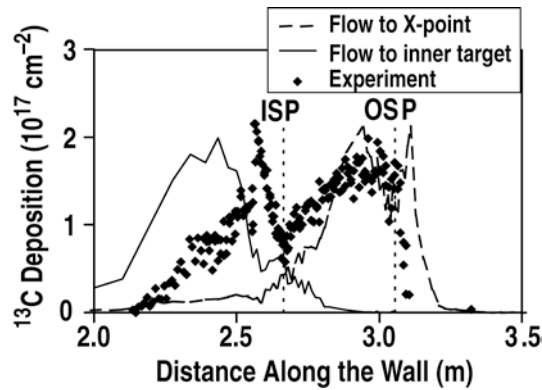

Fig. 3. ELM-dependent deposition hypothesis. Net deposition is the sum of the two results.

2.2. HYPOTHESIS 2: ELM-INDEPENDENT TRANSPORT

It is also possible that ELM influence on the transport pattern is not significant. In this case, the characteristic features of the ^{13}C deposition and magnitude have to be satisfied with a single set of transport assumptions. In this scenario, the plasma conditions and flow field were taken to be identical to the between-ELM case of Hypothesis 1. The only difference is that a radial pinch of 10 m/s was imposed instead of 20 m/s. This results in a dual peaked profile which is spread across the inner target and PFZ (Fig. 4). This is also a reasonable match to the general pattern and magnitude of the ^{13}C deposition.
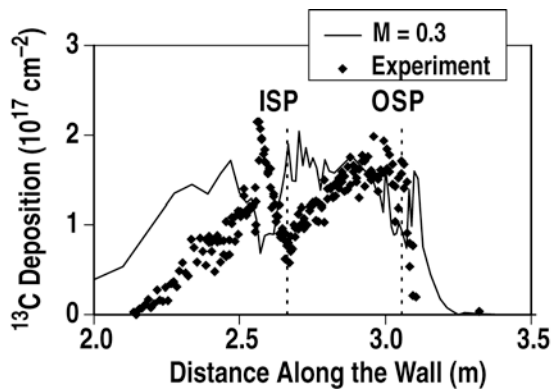

Fig. 4. ELM-independent deposition hypothesis. ^{13}C is deposited across the inner target and the PFZ using a single set of transport assumptions.

2.3. RESULTS WITH NO PARALLEL FLOW AND/OR RADIAL PINCH

A key finding of the analysis was that both parallel and radial transport are required in the simulation or the ^{13}C will not be deposited as measured experimentally. Figure 5 shows the deposition patterns resulting from cases with $M_{||} = 0.0$ and $M_{||} = 0.4$ in the SOL with no radial pinch applied in either case. If there is no parallel flow then there is no deposition at the inner target. If there is no radial pinch then the ^{13}C deposits at the inner edge of the inner target and along the inner wall; it does not deposit in the PFZ.
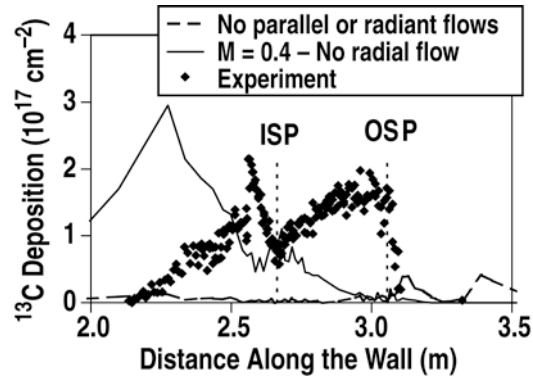

Fig. 5. Flow dependence of deposition. Results shown are for simulations with no parallel flow and no radial flow.

3. DISCUSSION

The foregoing simulations examine two hypotheses for the ^{13}C transport and deposition. It appears that either of these hypotheses could explain the experimentally observed deposition. Common to both hypotheses, however, are parallel flows in the SOL and a radial pinch. The assumption of the existence of a similar radial pinch was found necessary by Kirnev et al. [12] in EDGE2D code analysis in order to replicate the measured JET parallel flow pattern, specifically to obtain its closure via the radial pinch.

When comparing the deposition results between the L- and H-mode cases, the key difference requiring explanation is the deposition in the PFZ. In the simulations, the mechanism leading to the PFZ deposition is SOL flow which stops outside the inner divertor combined with a radial pinch which moves the carbon towards the separatrix. The flow deposits particles far enough from the targets that they enter the PFZ either as ions via cross field diffusion or as recombined neutrals. Once in the PFZ, the impurity particles deposit on the PFZ tiles primarily as neutrals. What could explain the difference in the flow pattern between low-density L- and high-density H-modes? Although the inner divertor plasma is detached in both the L- and H-mode experiments with temperatures less than 1 eV – the cold plasma region in the high density H-mode appears to extend all the way to the X-point region, while in the low density L-mode experiment it remains much closer to the target. This picture is supported by the good plasma reconstruction matches to hydrogen spectroscopic data as well as a limited number of DTS measurements in the inner divertor plasma near the X-point. It appears that parallel flows only extend as far as the start of the region of significant detachment and plasma recombination in the inner divertor. The significantly greater level of detachment in the high-density H-mode inner divertor causes the SOL flow pattern to be different with parallel flows stopping, at least for part of the ELM cycle, near the X-point region. In the simulations, this change in SOL flow leads to the ^{13}C deposition in the PFZ.

It is important to note that matching the deposition in the PFZ is not sufficient by itself to greatly constrain the magnitude of the parallel flow in the SOL. Simulations showed similar deposition in the PFZ over a wide range of Mach numbers. The key factor in the deposition is where this flow stops. All simulations in which a significant amount of C is transported near the X-point region result in C deposition in the PFZ. However, different parallel flow rates result in very different levels of C in the confined plasma. Future work will examine whether other diagnostic data are available to further constrain the simulation parameters.

As in the L-mode experiment, it appears that erosion and redeposition of the ^{13}C do not play a significant role in the final deposition pattern. Particularly sensitive analysis using proton-induced γ-ray emission of the ^{13}C enrichment on the surface shows no variations that might be indicative of regions experiencing erosion and redeposition for the tiles from the

inner target and PFZ [13]. This simplifying aspect of the present experiment cannot be expected generally – though it does appear to be characteristic of detached divertor conditions.

Parallel SOL flows toward the inner target are a key element of all the simulations leading to ^{13}C deposition replicating the experimental measurements. Fast SOL flows have been seen in both L- and H-mode on many tokamaks [14,15]. However, TTV images of CII and CIII for this particular experiment cannot confirm the existence of these flows. Preliminary modeling of the spectroscopic emissions resulting from the ^{13}CH$_4$ breakup in the upper SOL indicate that, in the high density H-mode plasma conditions, spectroscopic measurements are expected to be much less sensitive to fast flows than in the low density L-mode. The magnitude of the emissions, the shape of the emissions and the separation between the CII and CIII emission peaks are all less sensitive to the flows.

The fact that the injection of the methane was toroidally symmetric greatly aided the interpretation of the C deposition, not least because the OEDGE analysis code, like most edge codes, is 2D.

4. CONCLUSIONS

Two hypotheses of ^{13}C transport have been examined. Either hypothesis can explain the observed ^{13}C deposition in both distribution and magnitude, within the experimental uncertainties. Regarding the role of ELMs: (a) it appears they do not significantly *erode* the ^{13}C deposits that form on the inner target or PFZ, for these high density conditions where the inner divertor is strongly detached, (b) it has not been possible, so far, to conclude whether ELMs play a significant role, via *transport*, in the observed ^{13}C deposition process.

In both of the transport scenarios examined, parallel SOL flows are required to transport the ^{13}C to the inner divertor region. If there is no parallel flow, the ^{13}C will not deposit in the inner divertor and PFZ. A radial pinch flow on the order of 10 to 20 m/s is required to transport the ^{13}C towards the separatrix in the inner SOL. The fast breakup of the ^{13}CH$_4$ at the edge of the plasma leaves the C ions too far from the separatrix to deposit where it is seen experimentally. Lack of either hypothesis — parallel flow and radial pinch — will not replicate the experimental results.

Modeling indicates that the deposition in the PFZ in the H-mode experiment is linked to the parallel transport in the SOL. Flows which stop near the X-point region allow the ^{13}C to enter the PFZ and ultimately deposit on the PFZ tiles. It is postulated that the parallel flow slows or stops in the region where the detached inner divertor plasma becomes very cold, with high density, strong plasma recombination and stagnant parallel flow.

REFERENCES

[1] P. Wienhold, H.G. Esser, D. Hildebrandt, et al., J. Nucl. Mater. **290-293** (2001) 362.

[2] J. Likonen, S. Lehto, J.P. Coad, et al., Fusion Engin. Design **66-68** (2003) 219.

[3] S.L. Allen, A.G. McLean, W.R. Wampler, et al., J. Nucl. Mater. **337-339** (2005) 30.

[4] J.D. Elder, P.C. Stangeby, D.G. Whyte, et al., J. Nucl. Mater. **337-339** (2005) 79.

[5] A.G. McLean, J.D. Elder, P.C. Stangeby, et al., J. Nucl. Mater. **337-339** (2005) 128.

[6] W.R. Wampler, S.L. Allen, A.G. McLean, et al., J. Nucl. Mater. **337-339** (2005) 134.

[7] W.R. Wampler, A.G. McLean, S.L. Allen, et al., "Transport and Deposition of ^{13}C From Methane Injection into Partially Detached Divertor H-mode Plasmas in DIII-D" to be presented at the 17th Plasma Surface Interactions in Controlled Fusion Devices, Hefei, China, 2006.

[8] P.C. Stangeby, J.D. Elder, J.A. Boedo, et al., J. Nucl. Mater. **313-316** (2003) 883.

[9] R.K. Janev and D. Reiter, Phys. Plasmas **9** (2002) 4071.

[10] R.K. Janev and D. Reiter: "Collision processes of hydrocarbon species in hydrogen plasmas: I. The methane family," Report FZ-Jülich Jül -3966, Forschungszentrum Jülich, Jülich Germany (Feb. 2002).

[11] S. Lisgo, P.C. Stangeby, J.D. Elder, et al., J. Nucl. Mater. **337-339** (2005) 256.

[12] Kirnev, et al., J. Nucl. Mater. **337–339** (2005) 271.

[13] D.G. Whyte, private communication.

[14] J.P. Coad, N. Bekris, J.D. Elder, et al., J. Nucl. Mater. **290–293** (2001) 224.

[15] N. Asakura, H. Takenaga, S. Sakurai, et al., Plasma Phys. Control. Fusion **44** (2002) 2101.

ACKNOWLEDGMENTS